

Triple points and phase transitions of *D*-dimensional dyonic AdS black holes with quasitopological electromagnetism in Einstein-Gauss-Bonnet gravity

Ping-Hui Mou(牟平辉), Qing-Quan Jiang(蒋青权), Ke-Jian He(何柯腱), Guo-Ping Li(李国平)

Citation: Chin. Phys. B, 2024, 33 (**6**): 060401. DOI: 10.1088/1674-1056/ad3342
Journal homepage: http://cpb.iphy.ac.cn; http://iopscience.iop.org/cpb

What follows is a list of articles you may be interested in

View of thermodynamic phase transition of the charged Gauss—Bonnet AdS black hole via the shadow

Ke-Jian He(何柯腱), Sen Guo(郭森), Zhi Luo(罗智), and Guo-Ping Li(李国平)
Chin. Phys. B, 2024, 33 (**4**): 040403. DOI: 10.1088/1674-1056/ad225d

Thermodynamics in a quantum corrected Reissner—Nordström—AdS black hole and its GUP-corrections

Jian-Jun Song(宋建君) and Cheng-Zhou Liu(刘成周)
Chin. Phys. B, 2024, 33 (**4**): 040402. DOI: 10.1088/1674-1056/ad1a8a

Shadow thermodynamics of AdS black hole with the nonlinear electrodynamics term

He-Bin Zheng(郑何斌), Ping-Hui Mou(牟平辉), Yun-Xian Chen(陈芸仙), and Guo-Ping Li(李国平)
Chin. Phys. B, 2023, 32 (**8**): 080401. DOI: 10.1088/1674-1056/acc806

Thermodynamics and weak cosmic censorship conjecture of charged AdS black hole in the Rastall gravity with pressure

Xin-Yun Hu(胡馨匀), Ke-Jian He(何柯健), Zhong-Hua Li(李中华), Guo-Ping Li(李国平)
Chin. Phys. B, 2020, 29 (**5**): 050401. DOI: 10.1088/1674-1056/ab7daa

Gravitational quasi-normal modes of static R^2 Anti-de Sitter black holes

Hong Ma(马洪), Jin Li(李瑾)
Chin. Phys. B, 2017, 26 (**6**): 060401. DOI: 10.1088/1674-1056/26/6/060401

Triple points and phase transitions of D-dimensional dyonic AdS black holes with quasitopological electromagnetism in Einstein–Gauss–Bonnet gravity

Ping-Hui Mou(牟平辉)[1], Qing-Quan Jiang(蒋青权)[1,†], Ke-Jian He(何柯腱)[2], and Guo-Ping Li(李国平)[1,‡]

[1] *School of Physics and Astronomy, China West Normal University, Nanchong* 637000, *China*
[2] *College of Physics, Chongqing University, Chongqing* 401331, *China*

(Received 14 December 2023; revised manuscript received 24 January 2024; accepted manuscript online 13 March 2024)

By considering the negative cosmological constant Λ as a thermodynamic pressure, we study the thermodynamics and phase transitions of the D-dimensional dyonic AdS black holes (BHs) with quasitopological electromagnetism in Einstein–Gauss–Bonnet (EGB) gravity. The results indicate that the small/large BH phase transition that is similar to the van der Waals (vdW) liquid/gas phase transition always exists for any spacetime dimensions. Interestingly, we then find that this BH system exhibits a more complex phase structure in 6-dimensional case that is missed in other dimensions. Specifically, it shows for $D = 6$ that we observed the small/intermediate/large BH phase transitions in a specific parameter region with the triple point naturally appeared. Moreover, when the magnetic charge turned off, we still observed the small/intermediate/large BH phase transitions and triple point only in 6-dimensional spacetime, which is consistent with the previous results. However, for the dyonic AdS BHs with quasitopological electromagnetism in Einstein–Born–Infeld (EBI) gravity, the novel phase structure composed of two separate coexistence curves observed by Li *et al.* [*Phys. Rev. D* **105** 104048 (2022)] disappeared in EGB gravity. This implies that this novel phase structure is closely related to gravity theories, and seems to have nothing to do with the effect of quasitopological electromagnetism. In addition, it is also true that the critical exponents calculated near the critical points possess identical values as mean field theory. Finally, we conclude that these findings shall provide some deep insights into the intriguing thermodynamic properties of the dyonic AdS BHs with quasitopological electromagnetism in EGB gravity.

Keywords: AdS black hole, phase transition, triple point

PACS: 04.70.Dy, 04.50.Kd, 05.70.Fh **DOI:** 10.1088/1674-1056/ad3342

1. Introduction

A black hole (BH), known for its strong gravity, has been regarded as a perfect object for testing general relativity. In recent years, the Laser Interferometer Gravitational Wave Observatory (LIGO) detected gravitational waves from binary BH mergers,[1,2] and the Event Horizon Telescope (EHT) collaboration released images of supermassive BHs at the centers of galaxy M87* and the Milky Way.[3–9] Since then, a great deal of interesting research has been attracted to work on gravitational waves[10–13] and BH shadows.[14–22] These studies do not only obtain some important theoretical results, but also strongly demonstrate the existence of BHs in our universe and successfully validate the predictions of general relativity. In fact, it has been demonstrated that a BH is a thermodynamic system, and it possess numerous interesting and important thermodynamic properties that the ordinary thermodynamic system does not have.[23–25] In particular, Hawking and Page in the early 1980s showed that there is a phase transition between a stable BH and thermal radiation in the Schwarzschild–AdS BH, which is known as the Hawking–Page phase transition.[26] The anti-de Sitter/conformal field theory (AdS/CFT) correspondence suggests that the thermodynamic of the BH in AdS space can be related to the thermodynamic of the dual strongly coupled conformal field theory in the boundary of AdS space.[27–29] Therefore, within the framework of AdS/CFT correspondence, Witten interpreted the Hawking–Page phase transition as a confinement/deconfinement phase transition of gauge field.[30] Thus, the phase transition, as an interesting property of BHs has been widely studied for a long time.[31–36]

Recently, thermodynamics of AdS BHs has been studied in the extended phase space. In this framework, the negative cosmological constant Λ is treated as the thermodynamic pressure of a BH, with its conjugate quantity being the thermodynamic volume of the BH.[37–43] Subsequently, by comparing with the liquidgas system, Kubizňák and Mann proved that the BH system has the similar features, such as the same oscillatory behavior of pressure–volume (P–V), critical exponents, and scaling relations.[44] Therefore, an accurate analogy has been established between the charged AdS BH and the vdW system.[44] This analogy has also been generalized to different types of AdS BHs, and then the later results show that the small/large BH phase transitions similar to the vdW liquid/gas phase transition are generally obtained in various

†Corresponding author. E-mail: qqjiangphys@yeah.net
‡Corresponding author. E-mail: gpliphys@yeah.net

© 2024 Chinese Physical Society and IOP Publishing Ltd

AdS BHs.[45–50] Afterwards, a series of interesting phase transitions were discovered in the extended phase space, which include the reentrant phase transition and the triple point.[51–64] For example, Wei *et al.* demonstrated that there are triple points in 6-dimensional GB AdS BHs,[53–55] and Frassino *et al.* found the reentrant phase transition in 3rd-order Lovelock gravity.[54] In the case of higher-order gravity theories, there are also multicritical phase transitions in AdS BHs, i.e., in higher-order Lovelock gravity.[65–67]

The extended gravity theories, including EGB gravity, have brought some new insights to study the property of BHs.[68–76] As a higher-order extension of Einstein gravity, the EGB gravity exhibits several striking features. In Ref. [69], Glavan introduced a rescaled GB coupling constant and defined the four-dimensional theory as a limit of $D \to 4$, thereby extended the Einstein–Hilbert action by incorporating the GB term. This framework bypasses the Lovelock theory and avoids Ostrogradsky instability.[69] Recently, some significant progresses have been made in the research of BHs in the background of EGB gravity.[70–76] For instance, in four-dimensional EGB gravity, there exist triple points in the Born–Infeld AdS BH.[60] These studies indicate that BHs in EGB gravity possess many interesting properties. On the other hand, the quasitopological electromagnetism is also regarded as an important and interesting object in the study of BHs.[77–81] Recently, Liu *et al.* proposed a new concept of quasitopological electromagnetism, and defined it as the square norm of the topological wedge product of Maxwell field strength of order k ($k \geqslant 2$).[77] In general, quasitopological terms have no effects on either the Maxwell equations or the energy-momentum tensor. Although they are known to have no effect on pure electric or magnetic Reissner–Nordström (RN) BHs, their influence on the dyonic BHs cannot be ignored. Later, Li *et al.* investigated the thermodynamics and phase transitions of the dyonic AdS BHs with quasitopological electromagnetism in EBI gravity.[82] The result shows that the triple points can be observed, as well as a novel phase structure composed of two separate coexistence curves. Obviously, quasitopological electromagnetism has a significant effect on the phase transitions of dyonic BHs.

Very recently, combining the quasitopological electromagnetism with EGB gravity, a solution of D-dimensional dyonic AdS BHs has been obtained.[83] Interestingly, the authors found that it is thermodynamically stable in certain regions, while unstable in others. Also, the shadow of this BH shows that the radius of the BH shadow decreases with the GB coupling constant α or the dimension D. Moreover, it shows that the GB coupling constant α and magnetic charge $Q_{\rm m}$ have some significant effects on energy emission rates, while other quantities have relatively small effects. Clearly, these studies mean that the dyonic AdS BHs with quasitopological electromagnetism in EGB gravity have many intriguing characteristics, which is worth investigating more deeply. In addition, although the AdS BHs with quasitopological electromagnetism in EBI gravity exhibit a rich variety of phase transitions, i.e., the triple point,[82] it remains unclear whether this types of BHs in EGB gravity also exhibit these interesting phase transitions. Therefore, in this paper we aim at studying the thermodynamics and phase transitions of the dyonic AdS BHs in EGB gravity. We hope that the results in current text can further reveal the thermodynamic characteristics of this BH and then further provide some new insights into understanding the effects of both EGB gravity and quasitopological electromagnetism on dyonic AdS BHs.

This paper is organized as follows. In Section 2, we review the D-dimensional dyonic AdS BHs with quasitopological electromagnetism in EGB gravity and study its thermodynamics. In Section 3, we investigate the phase transitions and phase diagrams of the D-dimensional dyonic AdS BHs. In Section 4, we calculate the critical exponents near the critical points. Section 5 concludes with a summary and discussion.

2. Thermodynamics of the D-dimensional dyonic AdS BHs

The action of D-dimensional EGB gravity minimally coupled to the quasitopological electromagnetism can be expressed as[83]

$$S_D = \frac{1}{16\pi}\int \mathrm{d}^D x\sqrt{-g}(\mathcal{R} - 2\Lambda + \alpha\mathcal{G} + \mathcal{L}_{\rm QE}), \tag{1}$$

where $\Lambda = -\frac{(D-1)(D-2)}{2l^2}$ is the cosmological constant in the AdS space, $\mathcal{G} = \mathcal{R}^2 - 4\mathcal{R}^{\mu\nu}\mathcal{R}_{\mu\nu} + \mathcal{R}^{\mu\nu\rho\sigma}\mathcal{R}_{\mu\nu\rho\sigma}$ is the GB term, α is the GB coupling constant with dimension [length]^2. The matter field is represented by the following quasitopological electromagnetism Lagrangian:

$$\mathcal{L}_{\rm QE} = -\left(\frac{1}{4}\mathcal{F}^2 + \frac{1}{2p!}\mathcal{H}^2 + \beta\mathcal{L}_{\rm int}\right) \tag{2}$$

with $p = D-2$, $\mathcal{F}^2 = \mathcal{F}_{\mu\nu}\mathcal{F}^{\mu\nu}$ and $\mathcal{H}^2 = \mathcal{H}_{\rho_1\cdots\rho_p}\mathcal{H}^{\rho_1\cdots\rho_p}$, and β is the coupling constant of the dimension [length]^2. The interaction term is given by

$$\mathcal{L}_{\rm int} = \delta^{\lambda_1\ldots\lambda_D}_{\gamma_1\ldots\gamma_D}\mathcal{F}_{\lambda_1\lambda_2}\mathcal{H}_{\lambda_3\ldots\lambda_D}\mathcal{F}^{\gamma_1\gamma_2}\mathcal{H}^{\gamma_3\cdots\gamma_D}. \tag{3}$$

The above action admits a BH solution with the form expressed as the following metric:

$$\mathrm{d}s^2 = -f(r)\mathrm{d}t^2 + f(r)^{-1}\mathrm{d}r^2 + r^2\mathrm{d}\Omega^2_{D-2}, \tag{4}$$

where $\mathrm{d}\Omega^2_{D-2}$ is the $(D-2)$-dimensional unit sphere. The metric function is given by

$$f(r)=1+\frac{r^2}{2\widetilde{\alpha}}\left(1-\sqrt{1+\frac{4\widetilde{\alpha}m}{r^{D-1}}+\frac{8\widetilde{\alpha}\Lambda}{(D-2)(D-1)}-\frac{2\widetilde{\alpha}}{(D-3)(D-2)r^{2D-4}}(Q_{\rm m}^2+Q_{\rm e}^2\mathcal{E})}\right), \tag{5}$$

with

$$\mathcal{E}={}_2F_1\left[1,\frac{D-3}{2(D-2)};\frac{7-3D}{4-2D};\frac{-8\beta Q_{\rm m}^2\Gamma(D-1)^2}{r^{2D-4}}\right] \tag{6}$$

being the hypergeometric function. Here, $\widetilde{\alpha}=(D-4)(D-3)\alpha$, $Q_{\rm e}$ and $Q_{\rm m}$ are the BH electric charge and magnetic charge, respectively. The parameter m is interpreted as the mass of the solution in a specific parameter space, which is the integration constant provided by the boundary conditions. Thus, the relevant Arnowitt–Deser–Misner (ADM) mass M is defined as[84]

$$M=\frac{(D-2)\mathcal{V}_{D-2}}{16\pi}m, \tag{7}$$

where $\mathcal{V}_{D-2}=2\pi^{\frac{D-1}{2}}/\Gamma(\frac{D-1}{2})$ is the volume of the $(D-2)$-dimensional unit sphere. Moreover, when the magnetic charge $Q_{\rm m}$ turns off, this BH will return to the charged GB AdS BH:[47]

$$f(r)=1+\frac{r^2}{2\widetilde{\alpha}}\left(1-\sqrt{1+\frac{64\pi\widetilde{\alpha}M}{(D-2)\mathcal{V}_{D-2}r^{D-1}}+\frac{8\widetilde{\alpha}\Lambda}{(D-2)(D-1)}-\frac{2\widetilde{\alpha}Q_{\rm e}^2}{(D-3)(D-2)r^{2D-4}}}\right). \tag{8}$$

In the extended phase space, the negative cosmological constant Λ is treated as the thermodynamic pressure $P=-\frac{\Lambda}{8\pi}$.[37] The BH horizon radius $r_{\rm h}$ is determined by the largest root of the equation $f(r_{\rm h})=0$. It can be obtained by solving this equation. Therefore, we can express the mass of BH in terms of the horizon radius $r_{\rm h}$ as

$$\begin{aligned}M=&\frac{P\pi^{\frac{D-1}{2}}r_{\rm h}^{D-1}}{\Gamma(\frac{D+1}{2})}+\frac{(D-2)\pi^{\frac{D-3}{2}}r_{\rm h}^{D-3}}{8\Gamma(\frac{D-1}{2})}\\&+\frac{\pi^{\frac{D-3}{2}}r_{\rm h}^{3-D}(Q_{\rm m}^2+Q_{\rm e}^2\mathcal{E}_{r_{\rm h}})}{16(D-3)\Gamma(\frac{D-1}{2})}+\frac{\pi^{\frac{D-3}{2}}r_{\rm h}^{D-5}\mathcal{N}_1}{8\Gamma(\frac{D-1}{2})},\end{aligned} \tag{9}$$

where

$$\begin{aligned}&\mathcal{E}_{r_{\rm h}}={}_2F_1\left[1,\frac{D-3}{2(D-2)};\frac{7-3D}{4-2D};\frac{-8\beta Q_{\rm m}^2\Gamma(D-1)^2}{r_{\rm h}^{2D-4}}\right],\\&\mathcal{N}_1=(D-4)(D-3)(D-2)\alpha.\end{aligned} \tag{10}$$

Further, based on the definition of Hawking temperature $T=\frac{f'(r_{\rm h})}{4\pi}$, the BH temperature can be obtained as

$$\begin{aligned}T=&\big\{[12+2D(D-5)+32P\pi r_{\rm h}^2+2D(D-5)r_{\rm h}^{-2}\mathcal{N}_1\\&-r_{\rm h}^{6-2D}Q_{\rm m}^2]\mathcal{N}_2-r_{\rm h}^6Q_{\rm e}^2\big\}/\big\{[8(D-2)\pi r_{\rm h}\\&+16\pi r_{\rm h}^{-1}\mathcal{N}_1]\mathcal{N}_2\big\},\end{aligned} \tag{11}$$

where

$$\mathcal{N}_2=r_{\rm h}^{2D}+8r_{\rm h}^4\beta Q_{\rm m}^2\Gamma(D-1)^2. \tag{12}$$

It is worth noting that BH mass in the extended phase space should be regarded as the enthalpy, instead of the internal energy of the system, i.e., $H\equiv M$. Therefore, the other thermodynamic quantities of BH, such as the thermodynamic volume V, entropy S, electric potential $\Phi_{\rm e}$, and magnetic potential $\Phi_{\rm m}$, can be calculated by

$$V=\left(\frac{\partial H}{\partial P}\right)_{S,Q_{\rm e},Q_{\rm m}}=\frac{2\pi^{\frac{D-1}{2}}r_{\rm h}^{D-1}}{(D-1)\Gamma(\frac{D-1}{2})}, \tag{13}$$

$$\begin{aligned}S=&\int_0^{r_h}T^{-1}\left(\frac{\partial H}{\partial r}\right)_{P,Q_{\rm e},Q_{\rm m}}{\rm d}r\\=&\frac{\pi^{\frac{D-1}{2}}r_{\rm h}^{D-2}[1+2(D-3)(D-2)\alpha r_{\rm h}^{-2}]}{2\Gamma(\frac{D-1}{2})},\end{aligned} \tag{14}$$

$$\Phi_{\rm e}=\left(\frac{\partial H}{\partial Q_{\rm e}}\right)_{S,P,Q_{\rm m}}=\frac{\pi^{\frac{D-3}{2}}r_{\rm h}^{3-D}Q_{\rm e}\mathcal{E}_{r_{\rm h}}}{8(D-3)\Gamma(\frac{D-1}{2})}, \tag{15}$$

$$\begin{aligned}\Phi_{\rm m}=&\left(\frac{\partial H}{\partial Q_{\rm m}}\right)_{S,P,Q_{\rm e}}\\=&\frac{\pi^{\frac{D-3}{2}}r_{\rm h}^{3-D}[2(D-2)Q_{\rm m}^2+(D-3)Q_{\rm e}^2(r_{\rm h}^{2D}\mathcal{N}_2^{-1}-\mathcal{E}_{r_{\rm h}})]}{16(D-3)(D-2)Q_{\rm m}\Gamma(\frac{D-1}{2})}.\end{aligned} \tag{16}$$

We treat α and β as novel thermodynamic variables by considering the dimensional characteristic of them. It is easy to verify that these thermodynamic quantities satisfy the differential form

$${\rm d}H=T{\rm d}S+\Phi_{\rm e}{\rm d}Q_{\rm e}+\Phi_{\rm m}{\rm d}Q_{\rm m}+\Phi_\alpha{\rm d}\alpha+\Phi_\beta{\rm d}\beta+V{\rm d}P, \tag{17}$$

where

$$\begin{aligned}\Phi_\alpha\equiv&\left(\frac{\partial H}{\partial\alpha}\right)_{S,P,Q_{\rm e},Q_{\rm m},\beta}\\=&\frac{\pi^{\frac{D-3}{2}}r_{\rm h}^{D-5}\mathcal{N}_1}{8\alpha\Gamma(\frac{D-1}{2})}-\frac{(D-3)(D-2)\pi^{\frac{D-1}{2}}r_{\rm h}^{D-4}T}{\Gamma(\frac{D-1}{2})}\end{aligned} \tag{18}$$

is the conjugate quantity to the GB coupling constant α, and

$$\Phi_\beta\equiv\left(\frac{\partial H}{\partial\beta}\right)_{S,P,Q_{\rm e},Q_{\rm m},\alpha}=\frac{\pi^{\frac{D-3}{2}}r_{\rm h}^{3-D}Q_{\rm e}^2(r_{\rm h}^{2D}\mathcal{N}_2^{-1}-\mathcal{E}_{r_{\rm h}})}{32(D-2)\beta\Gamma(\frac{D-1}{2})} \tag{19}$$

is the conjugate quantity to the coupling constant β. Moreover, the Smarr relation can be derived as

$$\begin{aligned}(D-3)H=&(D-2)TS-2PV+(D-3)\Phi_{\rm e}Q_{\rm e}\\&+(D-3)\Phi_{\rm m}Q_{\rm m}+2\alpha\Phi_\alpha+2\beta\Phi_\beta.\end{aligned} \tag{20}$$

The Gibbs free energy, which is a quantity measuring the global stability of BH system, is give as $G=H-TS$, i.e.,

$$G = 2(D-2)r_{\rm h}^{2D+2}\mathcal{N}_3 + 2r_{\rm h}^{2D}\mathcal{N}_1\mathcal{N}_3 + \frac{32P\pi r_{\rm h}^{2D+4}\mathcal{N}_3}{D-1} + \frac{r_{\rm h}^8(Q_{\rm m}^2+Q_{\rm e}^2\mathcal{E}_{r_{\rm h}})\mathcal{N}_3}{D-3} - \frac{[2(D-3)(D-2)\alpha+r_{\rm h}^2][(2r_{\rm h}^{2D}\mathcal{N}_4 - r_{\rm h}^8Q_{\rm m}^2)\mathcal{N}_2 - r_{\rm h}^{2D+8}Q_{\rm e}^2]\mathcal{N}_3}{[(D-2)r_{\rm h}^2+2\mathcal{N}_1]\mathcal{N}_2}, \tag{21}$$

where

$$\mathcal{N}_3 = \frac{\pi^{\frac{D-3}{2}}r_{\rm h}^{-5-D}}{16\Gamma(\frac{D-1}{2})},$$
$$\mathcal{N}_4 = 6r_{\rm h}^2 + D(D-5)r_{\rm h}^2 + 16P\pi r_{\rm h}^4 + (D-5)\mathcal{N}_1. \tag{22}$$

As is well known, the swallowtail behavior of the Gibbs free energy indicates the occurrence of a first-order phase transition in BH systems. Multiple swallowtails mean some rich varieties of phase transitions in the system, including the triple points. Therefore, in this paper, we study the phase transitions of BHs by analyzing the swallowtail behavior of the Gibbs free energy.

3. Phase transitions and phase diagrams of the *D*-dimensional dyonic AdS BHs

In this section, we would like to study the phase transitions and phase diagrams of the dyonic AdS BHs with quasitopological electromagnetism in dimensions $D = 4$, 5, 6 and 7 (the case of $D \geq 8$ is quite complex, and we will discuss it in our future work). Based on the equation of temperature, Eq. (11), the equation of state for BH system can be obtained as follows:

$$P = \frac{Q_{\rm m}^2}{32\pi r_{\rm h}^{2D-4}} - \frac{(D-4)(D-3)(D-2)(D-5-8\pi r_{\rm h}T)\alpha}{16\pi r_{\rm h}^4} + \frac{(D-2)(3-D+4\pi r_{\rm h}T)}{16\pi r_{\rm h}^2} + \frac{Q_{\rm e}^2}{32\pi r_{\rm h}^{2D-4}+256\pi\beta Q_{\rm m}^2\Gamma(D-1)^2}. \tag{23}$$

According to Ref. [44], the specific volume can be given as $v = \frac{4r_{\rm h}}{D-2}$, thereby the equation of state can be rewritten in the form of

$$P(v,T) = \frac{16(D-4)(D-3)[5-D+2(D-2)\pi vT]\alpha}{(D-2)^3\pi v^4} + \frac{2^{4D-13}(D-2)^{4-2D}v^{4-2D}Q_{\rm m}^2}{\pi} + \frac{3-D+(D-2)\pi vT}{(D-2)\pi v^2} + \frac{Q_{\rm e}^2}{2^{13-4D}(D-2)^{2D-4}\pi v^{2D-4}+256\pi\beta Q_{\rm m}^2\Gamma(D-1)^2}. \tag{24}$$

Evidently, there exists a direct proportionality between the specific volume v and horizon radius $r_{\rm h}$. Therefore, we will utilize the equation of state, i.e., Eq. (23), in the following calculations. In addition, due to the thermodynamic volume $V \propto r_{\rm h}^{D-1}$, the critical point can be determined by the conditions

$$\left(\frac{\partial P}{\partial r_{\rm h}}\right)_T = 0,\ \left(\frac{\partial^2 P}{\partial r_{\rm h}^2}\right)_T = 0;\ \text{or}\ \left(\frac{\partial T}{\partial r_{\rm h}}\right)_P = 0,\ \left(\frac{\partial^2 T}{\partial r_{\rm h}^2}\right)_P = 0. \tag{25}$$

Different from the Gibbs free energy G, the heat capacity with a constant pressure C_P, is a quantity used to describe the local thermodynamic stability of BHs. Specifically, a positive value of C_P indicates that the system is locally stable, while a negative value is local instability. At a fixed pressure P, the heat capacity C_P is defined as

$$C_P = T\left(\frac{\partial S}{\partial T}\right)_P. \tag{26}$$

Further, C_P can be also re-expressed as

$$C_P = T\left(\frac{\partial_{r_{\rm h}} S}{\partial_{r_{\rm h}} T}\right)_P \propto (\partial_{r_{\rm h}} T)_P^{-1}. \tag{27}$$

Here, we only considered the range of $T > 0$ and $S > 0$ in this paper. Therefore, it can be seen that the positive (negative) slopes of the BH branches on the T–$r_{\rm h}$ plane correspond to the thermodynamically stable (unstable) phases, wherein their corresponding heat capacity C_P being positive (negative). In the following, our attention will mainly focus on the phase transitions and phase diagrams. For convenience, we will take the case, i.e., the magnetic charge $Q_{\rm m} = 2$ and electric charge $Q_{\rm e} = 1$, as an example to further study the phase transitions and phase diagrams of the dyonic AdS BHs in this paper. Specifically, we will discuss the phase transitions and phase diagrams for different dimensions and different values of the coupling parameters (α and β).

3.1. For the 4-dimensional case

In this subsection, we would like to study the phase transitions and phase diagrams of the 4-dimensional dyonic AdS BH. According to Eqs. (23) and (25), we obtain the critical points for different values of GB coupling constant α and β as shown in Table 1.

From Table 1, one can see that each situation has either one critical point or no critical point. Specifically, there is no critical point present in the region as long as $\beta \geqslant 1$, no matter what the value of α is. The critical points change slightly with the β, while is hardly changed with α. Since there is only one critical point for different values of parameters α and β, we can predicate that the BH system only exhibits single phase structure in 4-dimensional case. For convenience, we take $\alpha = 0.5$ and $\beta = 0.1$ as an example to study the phase transitions of BHs, where the critical point reads

$$T_{\rm c} = 0.0433165,\ \ P_{\rm c} = 0.0033158. \tag{28}$$

To analyze the behaviors of temperature T with respect to $r_{\rm h}$ and Gibbs free energy G with respect to T, we plot Figs. 1(a) and 1(b) by considering some acceptable of P, i.e., $P = 0.001$, 0.002, 0.0033158, and 0.005.

Table 1. Critical points for different values of coupling constants α and β, for dimension $D = 4$.

α	β	(T_c, P_c)	α	β	(T_c, P_c)
0.01	0.01	(0.04331644704, 0.003316488235)	0.1	0.01	(0.04331644704, 0.003316488235)
0.01	0.05	(0.04331648727, 0.003315881743)	0.1	0.05	(0.04331648727, 0.003315881743)
0.01	0.1	(0.04331648854, 0.003315804969)	0.1	0.1	(0.04331648854, 0.003315804969)
0.01	0.5	(0.04331648894, 0.003315743396)	0.1	0.5	(0.04331648894, 0.003315743396)
0.01	0.9	(0.04331648895, 0.003315736546)	0.1	0.9	(0.04331648895, 0.003315736546)
0.01	1	–	0.1	1	–
0.5	0.01	(0.04331644704, 0.003316488235)	1	0.01	(0.04331644704, 0.003316488235)
0.5	0.05	(0.04331648727, 0.003315881743)	1	0.05	(0.04331648727, 0.003315881743)
0.5	0.1	(0.04331648854, 0.003315804969)	1	0.1	(0.04331648854, 0.003315804969)
0.5	0.5	(0.04331648894, 0.003315743396)	1	0.5	(0.04331648894, 0.003315743396)
0.5	0.9	(0.04331648895, 0.003315736546)	1	0.9	(0.04331648895, 0.003315736546)
0.5	1	–	1	1	–
10	0.01	(0.04331644704, 0.003316488235)	50	0.01	(0.04331644704, 0.003316488235)
10	0.05	(0.04331648727, 0.003315881743)	50	0.05	(0.04331648727, 0.003315881743)
10	0.1	(0.04331648854, 0.003315804969)	50	0.1	(0.04331648854, 0.003315804969)
10	0.5	(0.04331648894, 0.003315743396)	50	0.5	(0.04331648894, 0.003315743396)
10	0.9	(0.04331648895, 0.003315736546)	50	0.9	(0.04331648895, 0.003315736546)
10	1	–	50	1	–

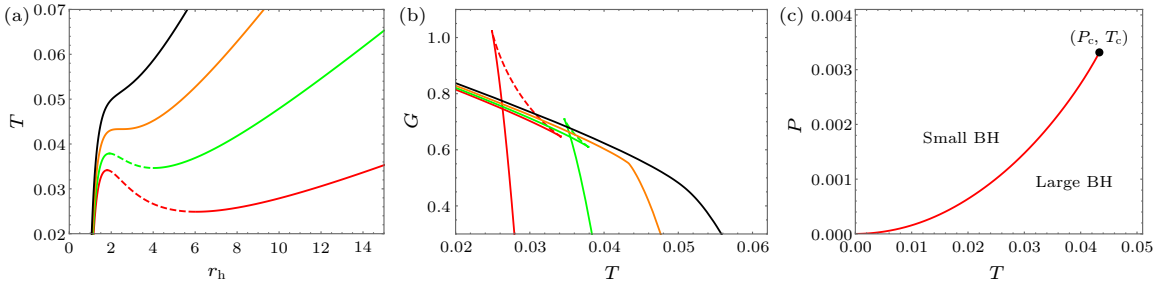


Fig. 1. (a) Temperature T vs. r_h. (b) Gibbs free energy G vs. T. The red, green, orange and black isobaric curves in (a) and (b) correspond to $P = 0.001$, 0.002, 0.0033158 and 0.005, respectively. Solid curves indicate stable branches, while dashed curves represent unstable branches. (c) Phase diagram for the 4-dimensional dyonic AdS BH when $\alpha = 0.5$ and $\beta = 0.1$.

Firstly, when $P < P_c$, it shows from Fig. 1(a) that two extremal points can be observed on both the red and green isobaric curves, which divide them into three branches: the small BH branch, the intermediate BH branch, and the large BH branch. Both small and large BH branches exhibit positive slope, implies that their heat capacity C_P is positive, and hence, they are thermodynamically stable, which is represented by solid curves in the figure. In contrast, the intermediate BH branch shows a negative slope, suggests that its heat capacity C_P is negative, thereby it is thermodynamic instability, which is represented by a dashed curve. Increasing the pressure to $P > P_c$, we observe that there is no extremal point for the black curve. This implies that the system has only one stable BH branch in this case.

Next, we will focus on the behaviors of Gibbs free energy presented in Fig. 1(b). It should be noted that Figs. 1(a) and 1(b) represent the same BH branchs, where the same color curves correspond to the same pressures. When $P < P_c$, both the red and green isobaric curves exhibit the swallowtail behavior, which indicates that a first-order small/large BH phase transition occurs. It is worth emphasizing that the nonsmooth points on the isobaric curves in the G–T diagram correspond to the extremal points on the isobaric curves in the T–r_h diagram, where dashed curves represent the negative heat capacity and solid curves denote the positive one. For the red and green isobaric curves, the system initially exhibits a small BH phase, and then gradually transforms into a large BH phase as the temperature T increases and passes through the swallowtail intersection. By comparing the red, green, and orange isobaric curves, we find that the swallowtail gradually becomes small and eventually disappears as the pressure P increases. With a progressive increase of pressure P, it shows that the extremal points of the temperature on the isobaric curve gradually are close to each other and finally overlapped at the critical pressure. When the pressure reaches the critical pressure P_c, the isobaric curve no longer exhibits swallowtail behavior. When $P > P_c$, the Gibbs free energy becomes a monotonic function of temperature, indicating that the system will not undergo any phase transitions. Finally, the coexistence curve of the small and large BH phases is plotted in Fig. 1(c). The P–T diagram indicates that the area above the coexistence curve corresponds to the small BH phase, while the area below it corresponds to the large BH phase. It is obvious that the pressure monotonically increases with temperature, and finally stops at the critical point (P_c, T_c) at which a second-order phase transition of BH occurs. This small/large BH phase transition is a typical

case, which is similar to the vdW liquid/gas phase transition. For other choice of α and β in Table 1, we have also studied the corresponding phase transitions in 4-dimensional case, and find that these phase transitions always are similar to the case of $\alpha = 0.5$ and $\beta = 0.1$.

3.2. For the 5-dimensional case

In this subsection, we would like to study the phase transitions and phase diagrams of the 5-dimensional dyonic AdS BH. Similarly, the critical points for different combinations of parameters are listed in Table 2.

Table 2. Critical points for different values of coupling constants α and β, for dimension $D = 5$.

α	β	(T_c, P_c)	α	β	(T_c, P_c)
0.01	0.01	(0.1617879212, 0.03277316929)	0.1	0.01	(0.1167835294, 0.01899568735)
0.01	0.1	(0.1617879212, 0.03277316929)	0.1	0.1	(0.1167835294, 0.01899568735)
0.01	0.5	(0.1617879212, 0.03277316929)	0.1	0.5	(0.1167835294, 0.01899568735)
0.01	1	(0.1617879212, 0.03277316929)	0.1	1	(0.1167835294, 0.01899568735)
0.01	10	(0.1617879212, 0.03277316929)	0.1	10	(0.1167835294, 0.01899568735)
0.01	50	(0.1617879212, 0.03277316929)	0.1	50	(0.1167835294, 0.01899568735)
0.5	0.01	(0.06346110823, 0.006193085877)	1	0.01	(0.04564111900, 0.003251240167)
0.5	0.1	(0.06346110823, 0.006193085877)	1	0.05	(0.04564111900, 0.003251240167)
0.5	0.5	(0.06346110823, 0.006193085877)	1	0.1	(0.04564111900, 0.003251240167)
0.5	1	(0.06346110823, 0.006193085877)	1	0.5	(0.04564111900, 0.003251240167)
0.5	10	(0.06346110823, 0.006193085877)	1	0.9	(0.04564111900, 0.003251240167)
0.5	50	(0.06346110823, 0.006193085877)	1	1	–
10	0.01	(0.01452778369, 0.0003315037716)	50	0.01	(0.006497455295, 0.00006631401)
10	0.05	(0.01452778369, 0.0003315037716)	50	0.05	(0.006497455295, 0.00006631401)
10	0.1	(0.01452778369, 0.0003315037716)	50	0.1	(0.006497455295, 0.00006631401)
10	0.5	(0.01452778369, 0.0003315037716)	50	0.5	(0.006497455295, 0.00006631401)
10	0.9	(0.01452778369, 0.0003315037716)	50	0.9	(0.006497455295, 0.00006631401)
10	1	–	50	1	–

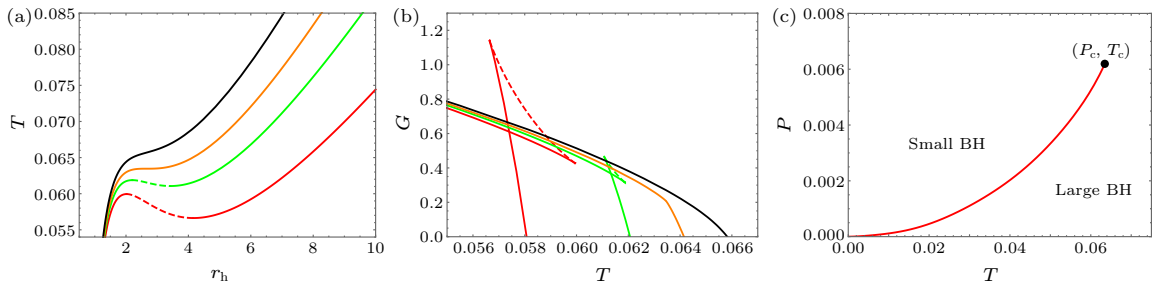


Fig. 2. (a) Temperature T vs. r_h. (b) Gibbs free energy G vs. T. The red, green, orange and black isobaric curves in (a) and (b) correspond to $P = 0.0045$, 0.0055, 0.00619309, and 0.007, respectively. (c) Phase diagram for the 5-dimensional dyonic AdS BH when $\alpha = 0.5$ and $\beta = 0.1$.

As can be seen from Table 2, there is only one critical point or no critical point for each choice of α and β. Specifically, the critical point does not exist in the parameter region where both α and β are all larger than or equal to 1 ($\geqslant 1$) simultaneously. When α is fixed, the critical point remains constant for different values of β. However, it will decrease with the increase of the α for a fixed β. For convenience, we choose $\alpha = 0.5$ and $\beta = 0.1$ as an example to study the phase transition of BHs. The critical point is given as

$$T_c = 0.0634611, \quad P_c = 0.00619309. \tag{29}$$

The behaviors of temperature T with respect to r_h and Gibbs free energy G with respect to T are plotted in Fig. 2.

When $P < P_c$, there are two extremal points on both the red and green isobaric curves in the T–r_h diagram, as well as two swallowtails along the isobaric curves in the G–T plot, as shown in Figs. 2(a) and 2(b). As $P > P_c$, this leads to the disappearance of both the extremal point of the temperature in the T–r_h diagram and the swallowtail behavior in the G–T plot, for their respective isobaric curves. The coexistence curve of the small and large BH phases is shown in Fig. 2(c). These results indicate a typical small/large BH phase transition, which is similar to the vdW liquid/gas phase transition. In addition, we have also found that the similar phase transitions always exist for other values of α and β in Table 2.

3.3. For the 6-dimensional case

In this subsection, we would like to study the phase transitions and phase diagrams of the 6-dimensional dyonic AdS BHs. Similarly, based on Eqs. (23) and (25), the critical points can be obtained as shown in Table 3.

Comparing Table 3 with Tables 1 and 2, we can see that

the results in dimension $D=6$ are more interesting than those in dimensions $D=4$ and 5. As $\alpha=0.1$, the system only exists one critical point whatever β is. However, three critical points can be observed for $\alpha \geqslant 0.5$ in Table 3. In the parameter region where $\alpha \geqslant 1$ and $\beta \geqslant 1$ simultaneously, all critical points disappear. It is easy to conclude that α has some stronger effect on the critical points by comparing with the β. Therefore, in general, we take $\alpha=0.1$ and $\beta=0.1$, $\alpha=0.5$ and $\beta=0.1$, and $\alpha=1$ and $\beta=0.1$ as three typical examples to study the phase transitions and phase diagrams of BHs in dimension $D=6$, and to further discuss the influence of α and β on BH phase transitions.

Table 3. Critical points for different values of coupling constants α and β, for dimension $D=6$.

α	β	(T_{c1}, P_{c1})	(T_{c2}, P_{c2})	(T_{c3}, P_{c3})
0.1	0.01	(0.1389283596, 0.02790310620)	–	–
0.1	0.1	(0.1389283596, 0.02790310620)	–	–
0.1	0.5	(0.1389283596, 0.02790310620)	–	–
0.1	1	(0.1389283596, 0.02790310620)	–	–
0.1	10	(0.1389283596, 0.02790310620)	–	–
0.1	50	(0.1389283596, 0.02790310620)	–	–
0.5	0.01	(0.06464171275, 0.006352744392)	(0.06473618157, 0.006536184200)	(0.06487209227, 0.00657574901)
0.5	0.1	(0.06464171275, 0.006352744392)	(0.06473618157, 0.006536184200)	(0.06487209227, 0.00657574901)
0.5	0.5	(0.06464171275, 0.006352744392)	(0.06473618157, 0.006536184200)	(0.06487209227, 0.00657574901)
0.5	1	(0.06464171275, 0.006352744392)	(0.06473618157, 0.006536184200)	(0.06487209227, 0.00657574901)
0.5	10	(0.06464171275, 0.006352744392)	(0.06473618157, 0.006536184200)	(0.06487209227, 0.00657574901)
0.5	50	(0.06464171275, 0.006352744392)	(0.06473618157, 0.006536184200)	(0.06487209227, 0.00657574901)
1	0.01	(0.04592800869, 0.003308303581)	(0.04593268003, 0.003311035759)	(0.05592461935, 0.05061099927)
1	0.1	(0.04592800869, 0.003308303581)	(0.04593268003, 0.003311035759)	(0.05592461935, 0.05061099927)
1	0.5	(0.04592800869, 0.003308303581)	(0.04593268003, 0.003311035759)	(0.05592461935, 0.05061099927)
1	1	–	–	–
10	0.01	(0.01452878785, 0.0003315722183)	(0.01452878790, 0.0003315722265)	(0.07964136252, 9.372787591)
10	0.1	(0.01452878785, 0.0003315722183)	(0.01452878790, 0.0003315722265)	(0.07964136252, 9.372787591)
10	0.5	(0.01452878785, 0.0003315722183)	(0.01452878790, 0.0003315722265)	(0.07964136252, 9.372787591)
10	1	–	–	–
50	0.01	(0.00649747332857, 0.0000663145587)	(0.00649747332858, 0.000066314558701)	(0.1182077162, 238.3354046)
50	0.1	(0.00649747332857, 0.0000663145587)	(0.00649747332858, 0.000066314558701)	(0.1182077162, 238.3354046)
50	0.5	(0.00649747332857, 0.0000663145587)	(0.00649747332858, 0.000066314558701)	(0.1182077162, 238.3354046)
50	1	–	–	–

3.3.1. Example I: $\alpha=0.1$ and $\beta=0.1$

In this subsubsection, when $\alpha=0.1$ and $\beta=0.1$, the critical point can be obtained, it is

$$T_c=0.138928, \quad P_c=0.0279031. \tag{30}$$

Figures 3(a) and 3(b) are devoted to illustrate the behavior of temperature T vs. r_h and Gibbs free energy G vs. T, respectively. It can be seen that when $\alpha=0.1$ and $\beta=0.1$ the BH system only undergoes a small/large BH phase transition. Also, we construct a phase diagram shown in Fig. 3(c). It is easy to find that the phase transitions and phase diagrams in this case is similar to those obtained in dimensions $D=4,5$.

Furthermore, we also plot the G–T and P–T diagrams for coupling constants $\alpha=0.1$ and $\beta=0.5$ as shown in Fig. 4. It can be seen that the system undergoes a small/large BH phase transition in this parameter region. By comparing Fig. 4 with Fig. 3, it can be observed that they are almost identical. This implies that the parameter β has a little effect on the BH phase transition in this case.

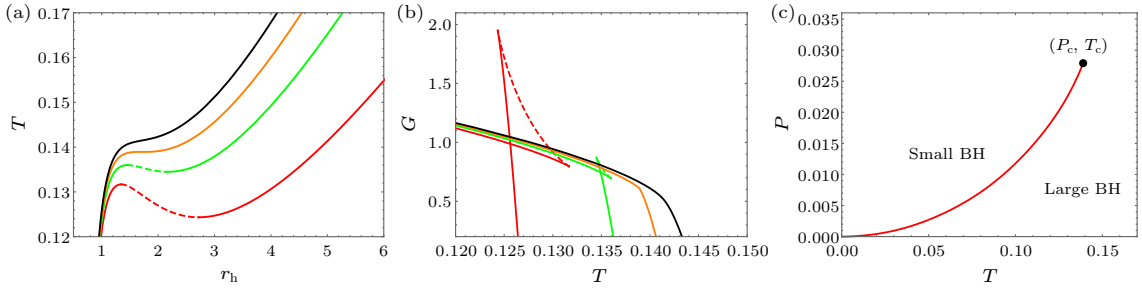


Fig. 3. (a) Temperature T vs. r_h. (b) Gibbs free energy G vs. T. The red, green, orange and black isobaric curves in (a) and (b) correspond to $P=0.02$, 0.025, 0.0279031, and 0.03, respectively. (c) Phase diagram for the 6-dimensional dyonic AdS BHs when $\alpha=0.1$ and $\beta=0.1$.

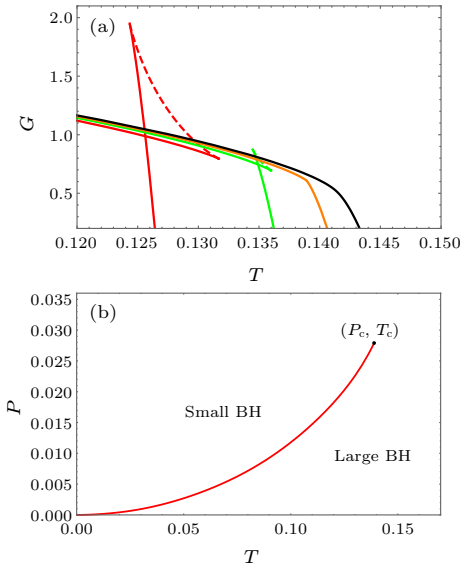


Fig. 4. (a) G vs. T. (b) Phase diagram for the 6-dimensional dyonic AdS BHs when $\alpha = 0.1$ and $\beta = 0.5$.

3.3.2. Example II: $\alpha = 0.5$ and $\beta = 0.1$

In this subsubsection, we set $\alpha = 0.5$ and $\beta = 0.1$ to study the phase transitions and phase diagrams of the BHs. In this case, three critical points can be obtained, i.e.,

$$T_{c1} = 0.0646417, \quad P_{c1} = 0.00635274, \tag{31}$$

$$T_{c2} = 0.0647362, \quad P_{c2} = 0.00653618, \tag{32}$$

$$T_{c3} = 0.0648721, \quad P_{c3} = 0.00657575. \tag{33}$$

Firstly, we will analyze the behavior of temperature T with respect to r_h. In Fig. 5(a), the temperature T is plotted as a function of r_h, where pressure is considered as a variable. When $P < P_{c1}$, the blue isobaric curve on the T–r_h diagram has two extremal points that divide it into three branches: the stable small BH branch, the unstable intermediate BH branch, and the stable large BH branch. For $P_{c1} < P < P_{c2}$, the red isobaric curve has four extremal points that divide it into five branches: the stable small BH branch, the unstable small BH branch, the stable intermediate BH branch, the unstable large BH branch, and the stable large BH branch. For the red isobaric curve, one can utilize Maxwell equal area laws to plot two pairs of equal area regions at pressure $P = P_t = 0.00646982$, as shown in Fig. 5(b). It should be noted that the two pairs of regions obtained by using Maxwell equal area laws have the same temperature $T = T_t = 0.0647085$. This indicates that the BH system undergoes two phase transitions at the same pressure and temperature. This result implies the existence of the triple point, where small, intermediate, and large BH phases can coexist simultaneously. When the pressure reaches P_{c2}, the BH system undergoes a second-order intermediate/large BH phase transition.

For $P_{c2} < P < P_{c3}$, two extremal points appear on the orange isobaric curve. As a result, three distinct branches can be observed: the stable intermediate BH branch, the unstable intermediate BH branch, and the stable large BH branch. This result suggests the occurrence of the intermediate/large BH phase transition in this pressure range. However, this first-order phase transition turns to a second-order phase transition as the pressure approaches P_{c3}. For $P > P_{c3}$, there are no extremal point on the gray isobaric curve, indicating that temperature T becomes a monotonic function of r_h, and thus there exists only one BH branch.

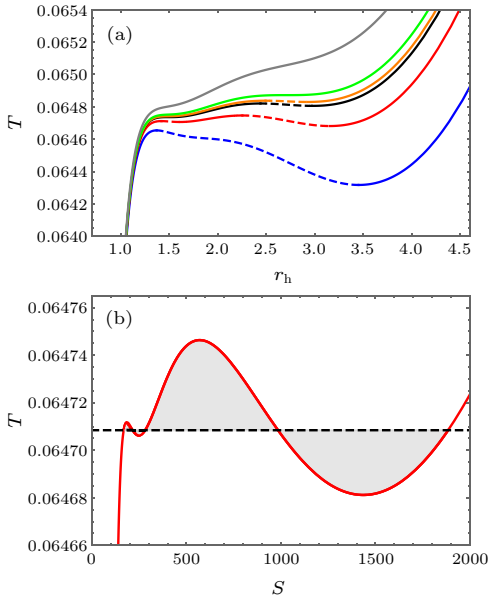


Fig. 5. (a) T vs. r_h. The blue, red, black, orange, green and gray isobaric curves correspond to $P = 0.0063$, 0.00646982, 0.00653618, 0.00655, 0.00657575, and 0.0067, respectively. (b) T–S diagram of two pairs of equal area regions at pressure $P = P_t = 0.00646982$. The horizontal line has a temperature $T = T_t = 0.0647085$.

Next, we will analyze the behavior of Gibbs free energy G with respect to T. Here, we have plotted the behavior of Gibbs free energy in Fig. 6. It is important to note that the nonsmooth points on the isobaric curves in the G–T diagram correspond to the extremal points on the isobaric curves in the T–r_h diagram. For $P < P_{c1}$, there is a swallowtail behavior in Fig. 6(a), suggesting the existence of a small/large BH phase transition. As the pressure increased to the range of $P_{c1} < P < P_t$, two swallowtail behaviors emerged in Fig. 6(b), which indicates the existence of three stable BH branches, and there seems to be two phase transitions. However, one of them will be suppressed and does not participate in the phase transition since its higher free energy. Therefore, there is only a small/large BH phase transition as the pressure in the region $P_{c1} < P < P_t$. When $P = P_t$, as shown in Fig. 6(c), the intersection of the two swallowtails occurs at the same position(P_t, T_t). This indicates that the three stable BH branches intersect at this point. Therefore, this result suggests that the triple point (T_t, P_t) exists for the current situation in this system, which means the small, intermediate and large BH phases can coexist simultaneously. For the case $P_t < P < P_{c2}$, as shown in Fig. 6(d),

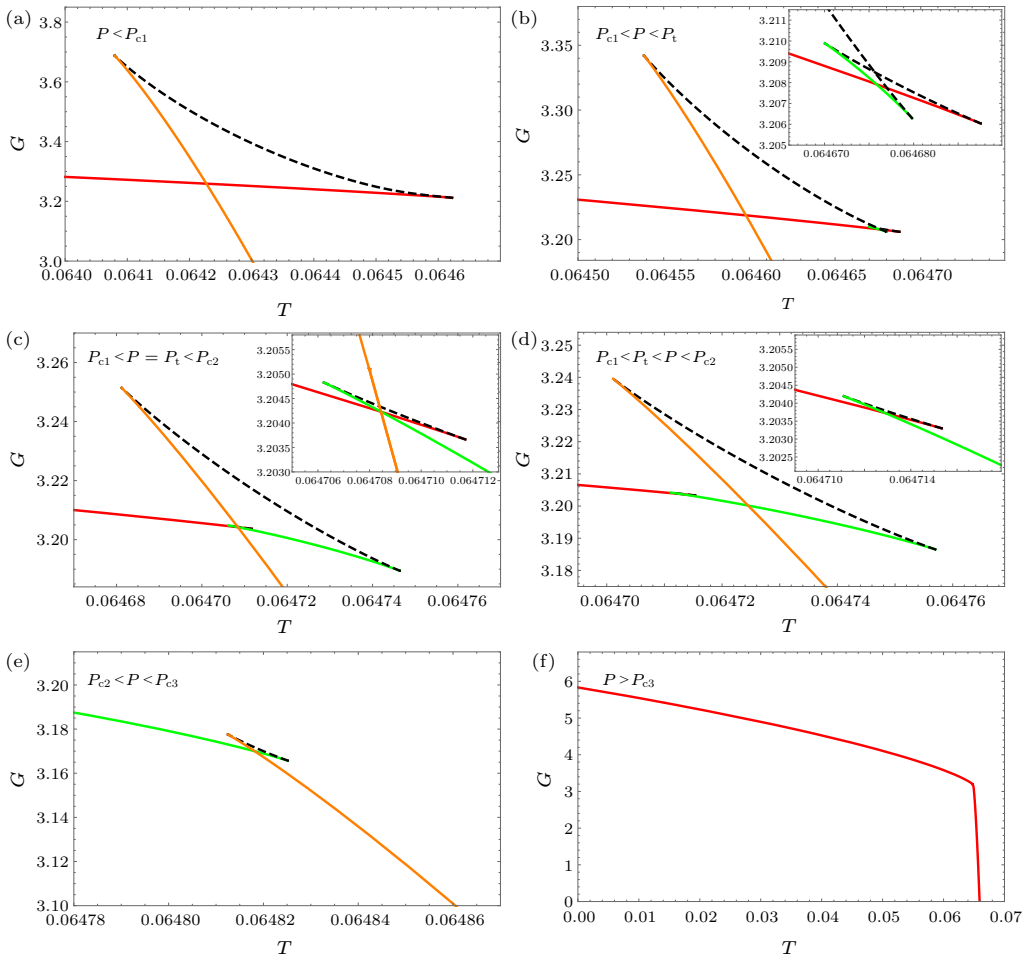


Fig. 6. G vs. T for (a) $P = 0.0062$, (b) $P = 0.0064$, (c) $P = P_t = 0.00646982$, (d) $P = 0.00648$, (e) $P = 0.00654$, and (f) $P = 0.0066$. The red, green, and orange curves represent small, intermediate, and large BHs, respectively.

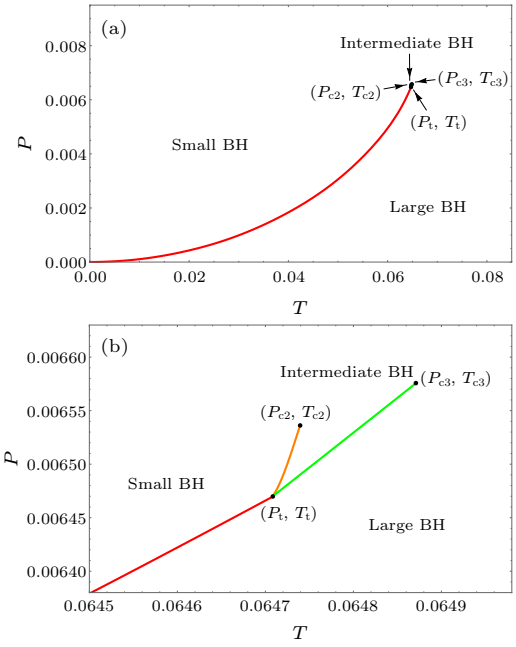


Fig. 7. Phase diagram for the 6-dimensional dyonic AdS BHs when $\alpha = 0.5$ and $\beta = 0.1$. (a) Entire phase diagram. (b) An enlarged view near the triple point (P_t, T_t).

we find that two swallowtails are also observed, and all three BH branches can participate in the phase transitions. This implies that at the same pressure but different temperatures, both the small/intermediate BH phase transition and the intermediate/large BH phase transition can occur simultaneously. As $P_{c2} < P < P_{c3}$, from Fig. 6(e), it shows that there is only one swallowtail, which indicates that only the intermediate/large BH phase transition presents. However, for $P > P_{c3}$, the Gibbs free energy G becomes a monotonic function of T, thereby no phase transition occurs in the system.

Finally, we construct the P–T phase diagram as shown in Fig. 7. Specifically, Fig. 7(a) is the global phase diagram, while Fig. 7(b) is a local one near the triple point (P_t, T_t). From the P–T phase diagram, it can be observed in current situation that when $P < P_t$, the system undergoes a small/large BH phase transition. At $P = P_t$, the small, intermediate, and large BH phases can coexist simultaneously. In the range $P_t < P < P_{c2}$, the system undergoes both the small/intermediate BH phase transition and the intermediate/large BH phase transition simultaneously. For $P_{c2} < P < P_{c3}$, the system only undergoes the intermediate/large BH phase transition.

In addition, we also investigate the phase transitions of BH for $\alpha = 0.5$ and $\beta = 50$. The results indicate that the triple point ($P_t = 0.006469822191382499, T_t =$

0.06470845191069557) for $\alpha = 0.5$ and $\beta = 50$ is almost identical to that obtained for $\alpha = 0.5$ and $\beta = 0.1$ ($P_t = 0.006469822191382416, T_t = 0.06470845191069545$), with an accuracy up to 13 significant digits. We plot the G–T diagram at the triple point and the P–T phase diagram near the triple point for $\alpha = 0.5$ and $\beta = 50$ in Fig. 8. By comparing Figs. 6 and 7 with Fig. 8, there is almost no difference for the G–T and P–T plots that can be observed. This finding implies that when $\alpha = 0.5$, the BH system always posses remarkably similar phase transitions, irrespective of the variations of β. This means that the parameter α plays a key role during the studying of the phase transition of BH in dimension $D = 6$.

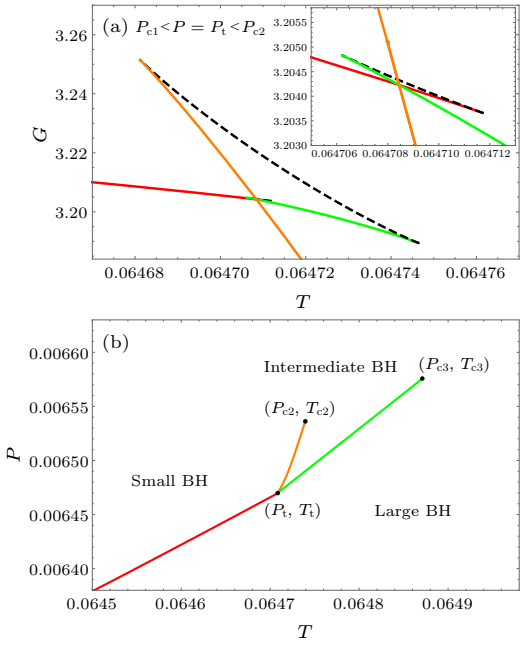


Fig. 8. (a) G vs. T. (b) Phase diagram for the 6-dimensional dyonic AdS BH when $\alpha = 0.5$ and $\beta = 50$.

3.3.3. Example III: $\alpha = 1$ and $\beta = 0.1$

In this subsubsection, by taking $\alpha = 1$ and $\beta = 0.1$, there also appears to be three critical points, i.e.,

$$T_{c1} = 0.0459280, \quad P_{c1} = 0.00330830, \tag{34}$$

$$T_{c2} = 0.0459327, \quad P_{c2} = 0.00331104, \tag{35}$$

$$T_{c3} = 0.0559246, \quad P_{c3} = 0.05061100. \tag{36}$$

Firstly, we plot the temperature T with respect to r_h in Fig. 9. When $P < P_{c1}$, the blue isobaric curve has two extremal points that divide it into three branches: the stable small BH branch, the unstable intermediate BH branch, and the stable large BH branch. When the pressure belongs to $P_{c1} < P < P_{c2}$, four extremal points appear for the red isobaric curve, which divides it into five branches: the stable small BH branch, the unstable small BH branch, the stable intermediate BH branch, the unstable large BH branch, and the stable large BH branch. For $P_{c2} < P < P_{c3}$, two extremal points appear for the orange isobaric curve, which means the existence of three BH branches. When $P > P_{c3}$, the gray isobaric curve does not exhibit any extremal points, which implies that there is only one BH branch.

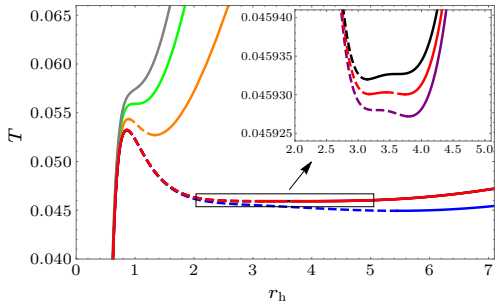


Fig. 9. Temperature T vs. r_h for $P = 0.003$ (blue curve), $P = 0.0033083$ (purple curve), $P = 0.0033097$ (red curve), $P = 0.00331104$ (black curve), $P = 0.025$ (orange curve), $P = 0.050611$ (green curve), and $P = 0.07$ (gray curve).

Next, we would like to study the behavior of Gibbs free energy. Therefore, the behavior of G with respect to T is plotted in Fig. 10. When $P < P_{c1}$, as shown in Fig. 10(a), the only one swallowtail indicates that the system undergoes a small/large BH phase transition. For $P_{c1} < P < P_{c2}$, as shown in Fig. 10(b), the two swallowtails seems indicates that there are two first-order phase transitions in the system. However, the intermediate BH branch is suppressed by the BH branch with lower free energy due to its higher free energy, so it cannot participate in the phase transitions. As a result, only a small/large BH phase transition occurs in this pressure range. When the pressure increases up to $P_{c2} < P < P_{c3}$, as shown in Fig. 10(c), the only one swallowtail indicates that the system only undergoes a small/large BH phase transition. Once the pressure exceeds P_{c3}, the swallowtail behavior disappears, which leads to the situation in which no phase transition occurs in the system. In addition, we present the phase diagram in Fig. 11, where the coexistence curve terminates at the critical point (P_{c3}, T_{c3}). One can obviously see that there has no triple point existing in current situation. To sum up, when $\alpha = 0.1$ and 1, the BH system only undergoes a small/large BH phase transition, which is very different from the case of $\alpha = 0.5$. Hence, it is true that the GB coupling constant α possess an important influence on the phase transition of the dyonic AdS BH.

In addition, we also investigate the phase transitions for $\alpha = 1$ and $\beta = 0.5$, for which the G–T diagram and P–T phase diagram are illustrated in Fig. 12. In this case, we only present the G–T diagram for the pressure of $P_{c1} < P = 0.0033097 < P_{c2}$, as it shows the fact that the intermediate BHs do not participate in the phase transition, resulting in only small/large BH phase transition occurs. In comparison of Figs. 10–12, it can be observed that their results are almost identical, which also implies that the parameter β has a little effect on the phase transition. Additionally, when we further study the phase transitions for $\alpha = 10$ and $\alpha = 50$, it is true that the corresponding

results are similar to that of $\alpha = 1$, where only the small/large BH phase transition occurs and β also has a little effect on it.

Finally, combined with the above results obtained in three examples ($\alpha = 0.1$ and $\beta = 0.1$; $\alpha = 0.5$ and $\beta = 0.1$; $\alpha = 1$ and $\beta = 0.1$), it can be concluded that in the context of 6-dimensional case, the GB coupling constant α has a strong effect on the phase transition of BHs, while β has a weaker one.

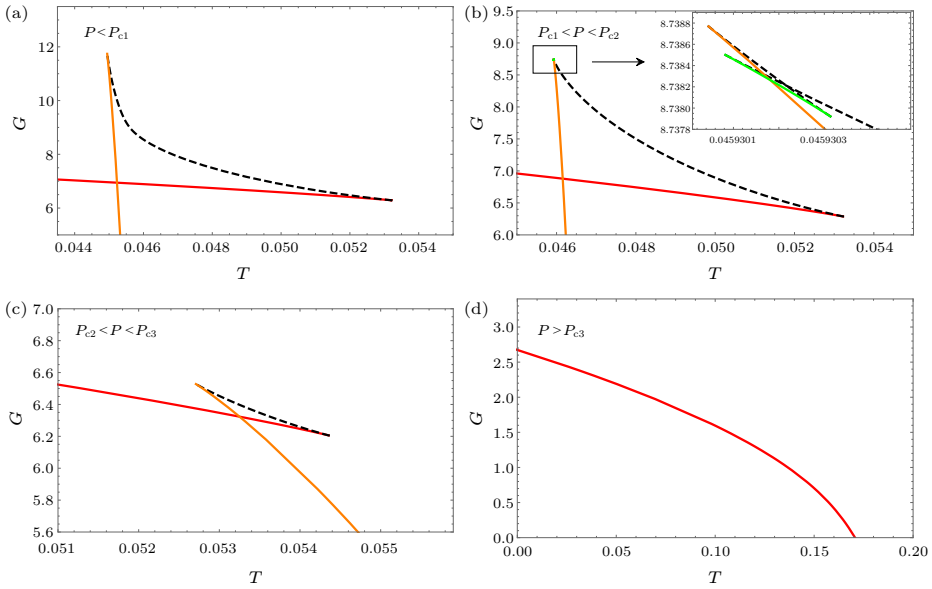


Fig. 10. Gibbs free energy G vs. T for (a) $P = 0.003$, (b) $P = 0.0033097$, (c) $P = 0.025$, and (d) $P = 0.07$. The red, green, and orange curves represent small, intermediate, and large BHs, respectively.

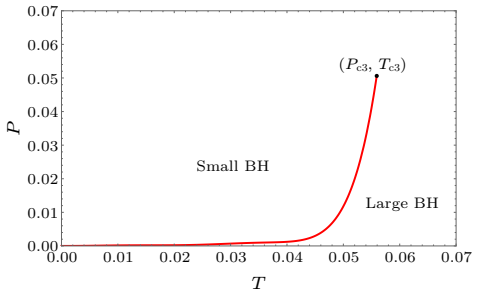


Fig. 11. Phase diagram for the 6-dimensional dyonic AdS BHs for $\alpha = 1$ and $\beta = 0.1$.

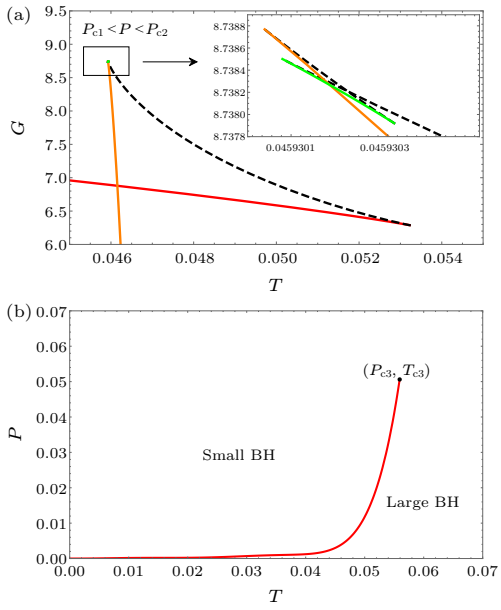


Fig. 12. (a) G vs. T. (b) Phase diagram for the 6-dimensional dyonic AdS BH when $\alpha = 1$ and $\beta = 0.5$.

In addition, when the magnetic charge turned off, we find that the small/intermediate/large BH phase transition still occurs only in 6-dimensional spacetime but is absent in the other dimensions. Therefore, we would like to study the phase transition when the magnetic charge turned off in 6-dimensional spacetime. In a particular parameter space ($D = 6$, $Q_e = 2$ and $\alpha = 0.5$) (In fact, when the magnetic charge turned off, the metric (5) is reduced to the form (8) which is the same as that in Ref. [47], but has a minute difference from that in Ref. [53]. Therefore, the triple point in this case occurs at $D = 6$, $Q_e = 2$, and $\alpha = 0.5$, which is also somewhat different from that in Ref. [53]. However, the main conclusion that the triple point observed in 6 dimensions is consistent with that in Ref. [53]), there are three critical points that can be obtained, which are

$$T_{c1} = 0.0646417, \quad P_{c1} = 0.00635274, \tag{37}$$

$$T_{c2} = 0.0647362, \quad P_{c2} = 0.00653618, \tag{38}$$

$$T_{c3} = 0.0648721, \quad P_{c3} = 0.00657575. \tag{39}$$

The behavior of the Gibbs free energy G with respect to T is illustrated in Fig. 13(a), and the P–T phase diagrams are plotted in Figs. 13(b) and 13(c). When the pressure takes a specific value of $P = P_t = 0.00646982$, it is observed that the small, intermediate, and large BH branches intersect at a point, which implies that there is a small/intermediate/large BH phase transition occurring. As a result, a triple point, where small, intermediate, and large BH phases coexist, i.e., ($P_t = 0.00646982$,

$T_t = 0.0647085$), can be observed in the P–T phase diagram. This is consistent with the previous results, as well as with the results of the GB AdS BHs,[53–55] where the triple points are observed only in 6-dimensional spacetime.

3.4. For the 7-dimensional case

In this subsection, we would like to study the phase transitions and phase diagrams of the 7-dimensional dyonic AdS BH. In a similar way, the critical points can be obtained, as listed in Table 4.

Table 4. Critical points for different values of coupling constants α and β, when the dimension $D = 7$.

α	β	(T_c, P_c)	α	β	(T_c, P_c)
0.01	0.01	(0.3468615086, 0.1399764527)	0.1	0.01	(0.1536583170, 0.04142045303)
0.01	0.1	(0.3468615086, 0.1399764527)	0.1	0.1	(0.1536583170, 0.04142045303)
0.01	0.5	(0.3468615086, 0.1399764527)	0.1	0.5	(0.1536583170, 0.04142045303)
0.01	1	(0.3468615086, 0.1399764527)	0.1	1	(0.1536583170, 0.04142045303)
0.01	10	(0.3468615086, 0.1399764527)	0.1	10	(0.1536583170, 0.04142045303)
0.01	50	(0.3468615086, 0.1399764527)	0.1	50	(0.1536583170, 0.04142045303)
0.5	0.01	(0.1131229239, 0.2880911532)	1	0.01	–
0.5	0.1	(0.1131229239, 0.2880911532)	1	0.1	–
0.5	0.5	(0.1131229239, 0.2880911532)	1	0.5	–
0.5	1	(0.1131229239, 0.2880911532)	1	1	–
0.5	10	(0.1131229239, 0.2880911532)	1	10	–
0.5	50	(0.1131229239, 0.2880911532)	1	50	–
10	0.01	–	50	0.01	–
10	0.1	–	50	0.1	–
10	1	–	50	1	–
10	50	–	50	50	–

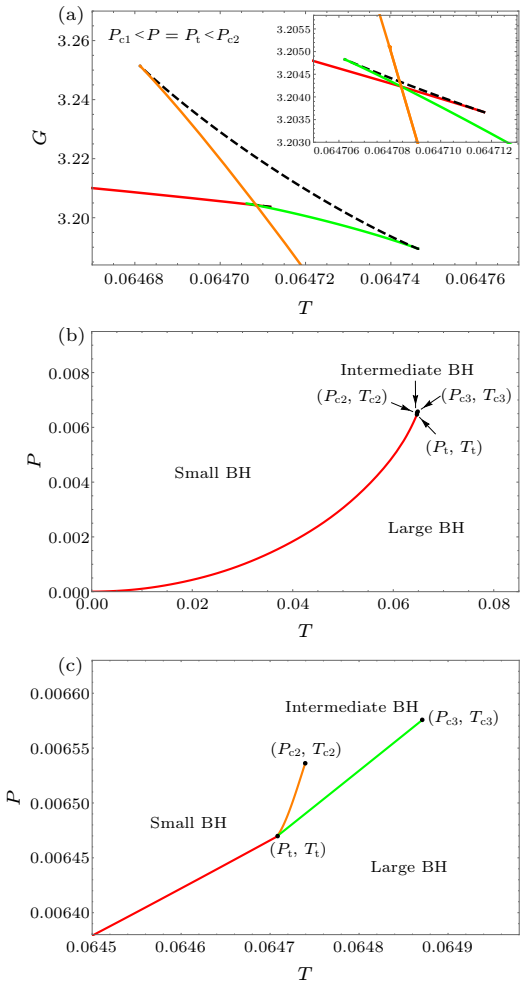


Fig. 13. (a) Gibbs free energy G vs. T. The red, green and orange curves represent small, intermediate, and large BHs, respectively. (b) P–T phase diagram. (c) An enlarged view near the triple point (P_t, T_t).

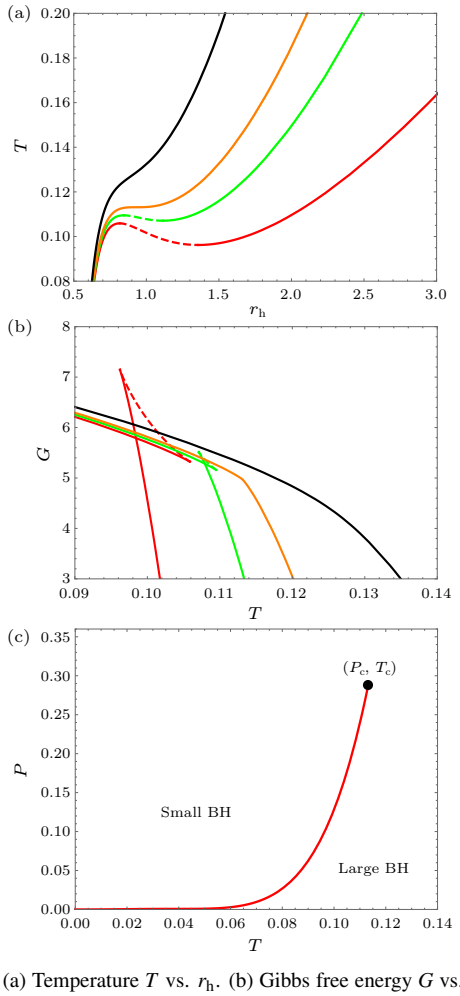


Fig. 14. (a) Temperature T vs. r_h. (b) Gibbs free energy G vs. T. The red, green, orange, and black curves in (a) and (b) correspond to pressures $P = 0.1$, 0.2, 0.288091, and 0.6, respectively. (c) Phase diagram for the 7-dimensional dyonic AdS BH when $\alpha = 0.5$ and $\beta = 0.1$.

In Table 4, when α is fixed and β varies, the critical points remain constant. However, when $\alpha \geqslant 1$, there is no critical point. It is no doubt that the BH system exhibits a single phase structure in dimension $D = 7$. In the case, i.e., $\alpha = 0.5$ and $\beta = 0.1$, the critical point is given as

$$T_{\rm c} = 0.113123, \quad P_{\rm c} = 0.288091. \tag{40}$$

The behavior of temperature T with respect to $r_{\rm h}$ and Gibbs free energy G with respect to T are plotted in Figs. 14(a) and 14(b), respectively. From Fig. 14, it can be seen that their behaviors are similar to those in dimensions of $D = 4$ and 5. When $P < P_{\rm c}$, the red and green isobaric curves in the T–$r_{\rm h}$ diagram are divided into three branches by two extremal points, and only one swallowtail appears in the G–T diagram for each curve. For $P = P_{\rm c}$, the system undergoes a second-order phase transition. When $P > P_{\rm c}$, the black isobaric curve in the T–$r_{\rm h}$ diagram becomes monotonic functions of $r_{\rm h}$. These results indicate that a small/large BH phase transition occurs in the BH system when $D = 7$. All of these results are similar to those of $D = 4$ and 5, and the corresponding phase diagram is shown in Fig. 14(c).

4. Critical exponents

In this section, we would like to calculate the critical exponents near the critical points. It is well known that critical exponents provide an effective way to characterize the behavior of physical quantities in the vicinity of the critical point. In general, these exponents are universal, and the details of the physical system would not affect it.

For simplicity, we define a few reduced parameters as follows:

$$t = \frac{T}{T_{\rm c}} - 1 = \tau - 1, \tag{41}$$

where $\tau = T/T_{\rm c}$ is the reduced thermodynamic temperature,

$$\omega = \frac{V}{V_{\rm c}} - 1 = \nu - 1, \tag{42}$$

where $\nu = V/V_{\rm c}$ is the reduced thermodynamic volume, and

$$p = \frac{P}{P_{\rm c}} \tag{43}$$

is the reduced thermodynamic pressure.

Next, let us review the definitions of the critical exponents α_1, β_1, γ, and δ near the critical point, which can be expressed as follows:[44]

(1) Exponent α_1 determines the behavior of the specific heat at constant volume,

$$C_{\rm V} = T\frac{\partial S}{\partial T}|_V \propto |t|^{-\alpha_1}. \tag{44}$$

(2) Exponent β_1 describes the behavior of the order parameter $\eta = V_{\rm l} - V_{\rm s}$ (the difference between the volumes of the coexisting large and small BHs) on a given isotherm

$$\eta = V_{\rm l} - V_{\rm s} \propto |t|^{\beta_1}. \tag{45}$$

(3) Exponent γ governs the behavior of the isothermal compressibility κ_T,

$$\kappa_T = -\frac{1}{V}\frac{\partial V}{\partial P}|_T \propto |t|^{-\gamma}. \tag{46}$$

(4) Exponent δ reflects the following behavior on the critical isotherm $T = T_{\rm c}$,

$$|P - P_{\rm c}| \propto |V - V_{\rm c}|^{\delta}. \tag{47}$$

Now we solve these critical exponents one by one. To calculate $C_{\rm V}$, we start from the definition of Helmholtz free energy $F(T,V) = G - PV$, and give the expression for Helmholtz free energy as

$$\begin{aligned} F(T,V) = {} & \frac{\pi^{\frac{D-3}{2}} r_{\rm h}^{D-3}(D-2-4\pi r_{\rm h}T)}{4(D-3)\Gamma(\frac{D-3}{2})} \\ & + \frac{\pi^{\frac{D-3}{2}} r_{\rm h}^{3-D}(Q_{\rm m}^2 + Q_{\rm e}^2\mathcal{E}_{r_{\rm h}})}{8(D-3)^2\Gamma(\frac{D-3}{2})} \\ & + \frac{(D-2)\pi^{\frac{D-3}{2}} r_{\rm h}^{D-5}(D-4-8\pi r_{\rm h}T)\alpha}{4\Gamma(\frac{D-3}{2})}. \end{aligned} \tag{48}$$

Thus, the entropy is

$$S(T,V) = -\left(\frac{\partial F}{\partial T}\right)_V = \frac{\pi^{\frac{D-1}{2}} r_{\rm h}^{D-2}[1 + 2(D-3)(D-2)\alpha r_{\rm h}^{-2}]}{2\Gamma(\frac{D-1}{2})}, \tag{49}$$

which is consistent with Eq. (14). Since S is independent of T, we have $C_{\rm V} = 0$, therefore the exponent $\alpha_1 = 0$. To compute the exponents β_1, γ and δ, we substitute the reduced parameters introduced in Eqs. (41)–(43) into Eq. (23) to derive the corresponding equation of state. In the vicinity of the critical point, the reduced pressure can be expressed as

$$p = A_0 + A_1\omega + A_2\omega^2 + A_3\omega^3 + B_0 t + B_1 t\omega + \mathcal{O}(t\omega^2, \omega^4). \tag{50}$$

The values of the expanded coefficients in Eq. (50) are calculated for various dimensions D, GB coupling constant α, and coupling constant β. The corresponding results are listed in Table 5.

As shown in Table 5, coefficient $A_0 = 1$, coefficient B_0 is positive, while coefficients A_3 and B_1 are negative. It is worth noting that coefficients A_1 and A_2 are absent in our BH system, hence they are not listed in the table. Therefore, we can reexpress the reduced pressure as

$$p = 1 + A_3\omega^3 + B_0 t + B_1 t\omega + \mathcal{O}(t\omega^2, \omega^4). \tag{51}$$

Under the condition of fixing $t < 0$, differentiating the reduced pressure in Eq. (51) yields

$$\mathrm{d}p = (3A_3\omega^2 + B_1 t)\,\mathrm{d}\omega. \tag{52}$$

In addition, the volumes of the coexisting small and large BHs are denoted by $\omega_{\rm s}$ and $\omega_{\rm l}$, respectively. The application of Maxwell equal area law gives

$$\int_{\omega_{\rm s}}^{\omega_{\rm l}} \omega(3A_3\omega^2+B_1 t)\,{\rm d}\omega = 0. \tag{53}$$

Moreover, the coexisting small and large BHs satisfy the equation of state, which is expressed as

$$p = 1+A_3\omega_{\rm s}^3+B_0 t+B_1 t\omega_{\rm s} = 1+A_3\omega_{\rm l}^3+B_0 t+B_1 t\omega_{\rm l}. \tag{54}$$

By solving Eqs. (53) and (54), we get $\omega_{\rm s} = -\omega_{\rm l} = -\sqrt{B_1/A_3}\sqrt{-t}$. Therefore, the order parameter η satisfies

$$\eta = V_{\rm c}(\omega_{\rm l}-\omega_{\rm s}) = 2V_{\rm c}\sqrt{B_1/A_3}\sqrt{-t}, \tag{55}$$

which indicates that the exponent $\beta_1 = 1/2$. To compute the exponent γ, we differentiate Eq. (51), and then get

$$\left.\frac{\partial V}{\partial P}\right|_T = \frac{1}{B_1}\frac{V_{\rm c}}{P_{\rm c}}\frac{1}{t}+\mathcal{O}(\omega). \tag{56}$$

Thus,

$$\kappa_{\rm T} = -\frac{1}{V}\left.\frac{\partial V}{\partial P}\right|_T \propto -\frac{1}{B_1}\frac{V_{\rm c}}{P_{\rm c}}\frac{1}{t}, \tag{57}$$

which implies that the exponent $\gamma = 1$. Finally, by setting the reduced temperature $t = 0$ in Eq. (51), we obtain

$$p-1 = A_3\omega^3, \tag{58}$$

which indicates that the exponent $\delta = 3$. It can be easily verified that these critical exponents satisfy the following scaling laws of thermodynamics:

$$\begin{aligned}&\alpha_1+2\beta_1+\gamma = 2,\ \ \alpha_1+\beta_1(1+\delta) = 2,\\ &\gamma(1+\delta) = (2-\alpha_1)(\delta-1),\ \ \beta_1(\delta-1) = \gamma.\end{aligned} \tag{59}$$

In summary, after calculating the four critical exponents of our BH system, namely,

$$\alpha_1 = 0,\ \ \beta_1 = 1/2,\ \ \gamma = 1,\ \ \delta = 3, \tag{60}$$

we conclude that our BH has the same critical exponents which have also been obtained in the dyonic AdS BH in EBI gravity.[82] In fact, these critical exponents possess identical values which coincide with the mean field theory. This property is very important and it further greatly supports the results obtained in this paper.

Table 5. The values of the expanded coefficients in Eq. (50) for various D, α, and β.

D	α	β	A_0	A_3	B_0	B_1
4	0.5	0.1	1	−0.0493816	2.66660	−0.88887
5	0.5	0.1	1	−0.0184683	3.70884	−1.33622
6	0.1	0.1	1	−0.0118259	4.10056	−1.29675
6	0.5	0.1	1	−0.0190869	24.6504	−12.1297
6	0.5	0.1	1	−0.0031754	6.63092	−2.52051
6	1	0.1	1	−0.1408537	14.0260	−7.97729
6	1	0.1	1	−0.0013238	7.38146	−2.89173
7	0.5	0.1	1	−0.0903225	7.85837	−3.75320

5. Discussion and conclusion

In this work, we have investigated the thermodynamics and phase transitions of the dyonic AdS BHs with quasitopological electrodynamics in EGB gravity, where the negative cosmological constant Λ is regarded as the thermodynamic pressure of BH and its conjugate quantity is introduced as the thermodynamic volume of BH. Firstly, we treat the GB coupling constant α and coupling constant β as novel thermodynamic variables to verify the first law of thermodynamics and derive the corresponding Smarr relation in a more general extended phase space. Then, we study the phase transitions by analyzing the characteristics of temperature and Gibbs free energy for the dyonic AdS BHs. Specifically, we investigate the phase transitions and phase diagrams for different dimensional cases, i.e., $D = 4$, 5, 6 and 7.

In the 4-dimensional case, we observe a typical small/large BH phase transition that is similar to the vdW liquid/gas phase transition. Notably, we find that the coupling constant β has a stronger effect on the critical points in contrast to α. The BH phase transition for the 5-dimensional case is similar to the 4-dimensional one, but the effect of α on the critical points is larger than that of β, rather than a smaller one. Interestingly, we also discover the typical small/large BH phase transition for the 7-dimensional case, where α has a greater impact on the critical points by comparing with β. However, the critical points in the 6-dimensional case are more interesting than those in the 4-, 5-, and 7-dimensional cases. Specifically, one can see that three critical points are obtained in the parameter region of $\alpha \geqslant 0.5$, which implies that the system exhibits some richer phase behaviors. It can also be seen that α has a significant effect on the values of the critical points, while the effect of β is weaker. For convenience, by fixing $\beta = 0.1$, we take $\alpha = 0.1$, 0.5 and 1 as three typical examples to further study the phase transitions and phase diagrams of the dyonic AdS BHs. For $\alpha = 0.1$, we find that there is a typical small/large BH phase transition in this case. It shows for $\alpha = 0.5$ that the system undergoes the small/intermediate/large BH phase transitions, rather than the small/large BH phase transition. Also, the triple point where all three BH phases coexist is obtained, i.e., ($P_{\rm t} = 0.00646982$, $T_{\rm t} = 0.0647085$). In the case $\alpha = 1$, although we find three critical points in this system, there is only the small/large BH phase transition, thereby the triple point no longer exists. When $\alpha > 1$, i.e., $\alpha = 10$ and 50, the results show that the BH phase transition is similar to that obtained in the case of $\alpha = 1$. Meanwhile, it is true in 6-dimensional spacetime that the coupling constant with respect to quasitopological electrodynamics β almost has no influence on the critical points, as well as phase transitions. This implies that the effect of the

parameter α on the BH phase transition is larger than that of β in the 6-dimensional case for the dyonic AdS BHs. Finally, when the magnetic charge turns off, we study the BH phase transition and find that the small/intermediate/large BH phase transitions as well as the triple point are still only observed in six-dimensional spacetime.

Combined with the above results, we conclude that the dimensions D and the GB coupling constant α have a significant effect on the phase transition, while the coupling parameter β has a relatively smaller influence on the phase transition. Specifically, the BH phase transition is determined by the dimensions D, and $D = 6$ is the condition for the appearance of the triple point. This is consistent with the results in GB AdS BHs, where the triple points are observed only in the 6-dimensional spacetime.[53–55] In addition, as illustrated in Tables 2–4, the GB coupling constant α determines the number and value of critical points. As discussed above, in 6-dimensional spacetime, $\alpha = 0.5$ is a specific condition for the existence of a triple point. However, the coupling constant β only determines the presence or absence of critical points, but does not affect the values of the critical points. Therefore, it can be concluded that the effect of β on the phase transition is smaller than that of α. On the other hand, it is obvious in EGB gravity that we do not find the novel phase structure that is composed of two separate coexistence curves in EBI gravity.[82] This implies that this novel phase structure is closely related to gravity theories, and seems to have nothing to do with the effect of quasitopological electromagnetism.

Furthermore, after calculating the critical exponents near the critical points, we obtain $\alpha_1 = 0$, $\beta_1 = 1/2$, $\gamma = 1$, and $\delta = 3$. Clearly, the critical exponents share the same values as mean field theory, which is also fully consistent with that of other BH systems. Finally, we conclude that our results can provide some deep insights into the intriguing thermodynamic properties of dyonic AdS BHs with quasitopological electromagnetism in EGB gravity.

In addition, the holographic duality also provides a valuable approach for the study of the thermodynamics of AdS BHs.[85,86] Therefore, it is meaningful to further study and test the thermodynamics of dyonic AdS BHs in the framework of AdS/CFT correspondence, which may further reveal more interesting thermodynamic properties. This will be included in our future work.

Acknowledgments

This work was supported by the National Natural Science Foundation of China (Grant No. 11903025), the Starting Fund of China West Normal University (Grant No. 18Q062), the Sichuan Science and Technology Program (Grant No. 2023ZYD0023), the Sichuan Youth Science and Technology Innovation Research Team (Grant No. 21CXTD0038), and the Natural Science Foundation of Sichuan Province (Grant No. 2022NSFSC1833).

References

[1] Abbott B P, *et al.* (LIGO Scientific and Virgo) 2016 *Phys. Rev. Lett.* **116** 241103
[2] Abbott B P, *et al.* (LIGO Scientific and Virgo) 2016 *Phys. Rev. D* **94** 064035
[3] Akiyama K, Alberdi A, Alef W, *et al.* (Event Horizon Telescope) 2019 *Astrophys. J. Lett.* **875** L1
[4] Akiyama K, Alberdi A, Alef W, *et al.* (Event Horizon Telescope) 2019 *Astrophys. J. Lett.* **875** L2
[5] Akiyama K, Alberdi A, Alef W, *et al.* (Event Horizon Telescope) 2019 *Astrophys. J. Lett.* **875** L3
[6] Akiyama K, Alberdi A, Alef W, *et al.* (Event Horizon Telescope) 2019 *Astrophys. J. Lett.* **875** L4
[7] Akiyama K, Alberdi A, Alef W, *et al.* (Event Horizon Telescope) 2022 *Astrophys. J. Lett.* **930** L12
[8] Akiyama K, Alberdi A, Alef W, *et al.* (Event Horizon Telescope) 2022 *Astrophys. J. Lett.* **930** L13
[9] Akiyama K, Alberdi A, Alef W, *et al.* (Event Horizon Telescope) 2022 *Astrophys. J. Lett.* **930** L14
[10] Liu J, Cai R G and Guo Z K 2021 *Phys. Rev. Lett.* **126** 141303
[11] Cai R G, Fu C and Yu W W 2022 *Phys. Rev. D* **105** 103520
[12] Cai R G, Guo Z K, Hu B, Liu C, Lu Y, Ni W T, Ruan W H, Seto N, Wang G and Wu Y L 2023 arXiv:2305.04551 [gr-qc]
[13] Xu H, Chen S, Guo Y, Jiang J, Wang B, Xu J, Xue Z, Caballero R N, Yuan J and Xu Y, *et al.* 2023 *Res. Astron. Astrophys.* **23** 075024
[14] Gralla S E, Holz D E and Wald R M 2019 *Phys. Rev. D* **100** 024018
[15] Gralla S E, Lupsasca A and Marrone D P 2020 *Phys. Rev. D* **102** 124004
[16] Li G P and He K J 2021 *J. Cosmol. Astropart. Phys.* **06** 037
[17] Gan Q, Wang P, Wu H and Yang H 2021 *Phys. Rev. D* **104** 044049
[18] Zeng X X, He K J and Li G P 2022 *Sci. China Phys. Mech. Astron.* **65** 290411
[19] Hadar S, Kapec D, Lupsasca A and Strominger A 2022 *Class. Quantum Grav.* **39** 215001
[20] Wang H M, Lin Z C and Wei S W 2022 *Nucl. Phys. B* **985** 116026
[21] Hou Y, Zhang Z, Yan H, Guo M and Chen B 2022 *Phys. Rev. D* **106** 064058
[22] Chen S B, Jing J L, Qian W L and Wang B 2023 *Sci. China Phys. Mech. Astron.* **66** 260401
[23] Bardeen J M, Carter B and Hawking S W 1973 *Commun. Math. Phys.* **31** 161
[24] Bekenstein J D 1973 *Phys. Rev. D* **7** 2333
[25] Hawking S W 1975 *Commun. Math. Phys.* **43** 199
[26] Hawking S W and Page D N 1983 *Commun. Math. Phys.* **87** 577
[27] Maldacena J M 1998 *Adv. Theor. Math. Phys.* **2** 231
[28] Gubser S S, Klebanov I R and Polyakov A M 1998 *Phys. Lett. B* **428** 105
[29] Witten E 1998 *Adv. Theor. Math. Phys.* **2** 253
[30] Witten E 1998 *Adv. Theor. Math. Phys.* **2** 505
[31] Chamblin A, Emparan R, Johnson C V and Myers R C 1999 *Phys. Rev. D* **60** 064018
[32] Chamblin A, Emparan R, Johnson C V and Myers R C 1999 *Phys. Rev. D* **60** 104026
[33] Surya S, Schleich K and Witt D M 2001 *Phys. Rev. Lett.* **86** 5231
[34] Cho Y M and Neupane I P 2002 *Phys. Rev. D* **66** 024044
[35] Shen J, Wang B, Lin C Y, Cai R G and Su R K 2007 *J. High Energy Phys.* **2007** 037
[36] Cai R G, Kim S P and Wang B 2007 *Phys. Rev. D* **76** 024011
[37] Kastor D, Ray S and Traschen J 2009 *Class. Quant. Grav.* **26** 195011
[38] Dolan B P 2011 *Class. Quant. Grav.* **28** 235017
[39] Cvetic M, Gibbons G W, Kubiznak D and Pope C N 2011 *Phys. Rev. D* **84** 024037
[40] Dolan B P, Kastor D, Kubiznak D, Mann R B and Traschen J 2013 *Phys. Rev. D* **87** 104017
[41] Kastor D, Ray S and Traschen J 2010 *Class. Quant. Grav.* **27** 235014
[42] Castro A, Dehmami N, Giribet G and Kastor D 2013 *J. High Energy Phys.* **07** 164

[43] Mahmoud El-Menoufi B, Ett B, Kastor D and Traschen J 2013 *Class. Quant. Grav.* **30** 155003
[44] Kubizňák D and Mann R B 2012 *J. High Energy Phys.* **07** 033
[45] Gunasekaran S, Mann R B and Kubizňák D 2012 *J. High Energy Phys.* **11** 110
[46] Chen S B, Liu X F, Liu C Q and Jing J L 2013 *Chin. Phys. Lett.* **30** 060401
[47] Cai R G, Cao L M, Li L and Yang R Q 2013 *J. High Energy Phys.* **09** 005
[48] Mo J X and Liu W B 2014 *Phys. Rev. D* **89** 084057
[49] Zou D C, Liu Y and Wang B 2014 *Phys. Rev. D* **90** 044063
[50] Wei S W and Liu Y X 2015 *Phys. Rev. Lett.* **115** 111302
[51] Altamirano N, Kubizňák D and Mann R B 2013 *Phys. Rev. D* **88** 101502
[52] Altamirano N, Kubizňák D, Mann R B and Sherkatghanad Z 2014 *Class. Quant. Grav.* **31** 042001
[53] Wei S W and Liu Y X 2014 *Phys. Rev. D* **90** 044057
[54] Frassino A M, Kubizňák D, Mann R B and Simovic F 2014 *J. High Energy Phys.* **09** 080
[55] Wei S W and Liu Y X 2022 *Commun. Theor. Phys.* **74** 095402
[56] Kubizňák D, Mann R B and Teo M 2017 *Class. Quant. Grav.* **34** 063001
[57] Zhang M, Zou D C and Yue R H 2017 *Adv. High Energy Phys.* **2017** 3819246
[58] Dehyadegari A and Sheykhi A 2018 *Phys. Rev. D* **98** 024011
[59] Dehghani A, Hendi S H and Mann R B 2020 *Phys. Rev. D* **101** 084026
[60] Zhang C M, Zou D C and Zhang M 2020 *Phys. Lett. B* **811** 135955
[61] Cui Y Z, Xu W and Zhu B 2023 *Phys. Rev. D* **107** 044048
[62] Liu Y P, Cao H M and Xu W 2022 *Gen. Rel. Grav.* **54** 5
[63] Qu Y, Tao J and Yang H 2023 *Nucl. Phys. B* **992** 116234
[64] Bai N C, Song L and Tao J 2022 arXiv:2212.04341 [hep-th]
[65] Tavakoli M, Wu J and Mann R B 2022 *J. High Energy Phys.* **12** 117
[66] Wu J and Mann R B 2023 *Class. Quant. Grav.* **40** 06LT01
[67] Wu J and Mann R B 2023 *Phys. Rev. D* **107** 084035
[68] Ghosh S G, Amir M and Maharaj S D 2017 *Eur. Phys. J. C* **77** 530
[69] Glavan D and Lin C 2020 *Phys. Rev. Lett.* **124** 081301
[70] Eslam Panah B, Jafarzade K and Hendi S H 2020 *Nucl. Phys. B* **961** 115269
[71] Yang K, Gu B M, Wei S W and Liu Y X 2020 *Eur. Phys. J. C* **80** 662
[72] Lin Z C, Yang K, Wei S W, Wang Y Q and Liu Y X 2020 *Eur. Phys. J. C* **80** 1033
[73] Fernandes P G S 2020 *Phys. Lett. B* **805** 135468
[74] Singh D V, Singh B K and Upadhyay S 2021 *Annals Phys.* **434** 168642
[75] Yerra P K and Bhamidipati C 2022 *Phys. Lett. B* **835** 137591
[76] Singh D V, Bhardwaj V K and Upadhyay S 2022 *Eur. Phys. J. Plus* **137** 969
[77] Liu H S, Mai Z F, Li Y Z and Lü H 2020 *Sci. China Phys. Mech. Astron.* **63** 240411
[78] Cisterna A, Giribet G, Oliva J and Pallikaris K 2020 *Phys. Rev. D* **101** 124041
[79] Lei Y Q, Ge X H and Ran C 2021 *Phys. Rev. D* **104** 046020
[80] Cisterna A, Henríquez-Báez C, Mora N and Sanhueza L 2021 *Phys. Rev. D* **104** 064055
[81] Barrientos J and Mena J 2022 *Phys. Rev. D* **106** 044064
[82] Li M D, Wang H M and Wei S W 2022 *Phys. Rev. D* **105** 104048
[83] Sekhmani Y, Lekbich H, El Boukili A and Sedra M B 2022 *Eur. Phys. J. C* **82** 1087
[84] Ghosh S G, Papnoi U and Maharaj S D 2014 *Phys. Rev. D* **90** 044068
[85] Ahmed M B, Cong W, Kubizňák D, Mann R B and Visser M R 2023 *Phys. Rev. Lett.* **130** 181401
[86] Ahmed M B, Cong W, Kubizňák D, Mann R B and Visser M R 2023 *J. High Energy Phys.* **08** 142